Lithium Zincates

DOI: 10.1002/anie.200901587

Solvent-Separated and Contact Ion Pairs of Parent Lithium Trimethyl Zincate**

*S. Merkel, D. Stern, J. Henn, and D. Stalke**

Bimetallic reagents, which are composed of one alkali metal ion, a second metal atom (Zn, Al, or Mg), and variable ligands have gained much attention over the last few years since they show a reactivity pattern that easily outperforms simple monometallic species.[1] Especially zincate complexes, although known to chemists for more than 150 years,[2] recently have been discovered to metalate substituted aromatic substrates at positions that can be reached neither by common organolithium nor by organomagnesium compounds alone. In their pioneering work, Mulvey and co-workers introduced the *meta* deprotonation into aromatic chemistry, complementing the established directed *ortho* metalation (DoM) by Snieckus and co-workers.[3] They were able to metalate the previously inaccessible *meta* position of *N*,*N*-dimethylaniline employing the amido zincate [(tmeda)Na(μ-*t*Bu)(μ-tmp)Zn*t*Bu)][4] and of toluene using [(tmeda)Na(μ-Bu)(μ-tmp)Mg(tmp)][5] (tmeda = tetramethylethylenediamine; tmp = tetramethylpiperidide). Another aspect is the smooth zincation of many substituted aromatics for which the traditionally used organolithium compounds fail because of their incompatibility with many functional groups.[6] These advantages of ate complexes over their monometallic congeners have been accredited to synergistic effects. In their milestone paper on alkali-metal organics in 1917,[7] Schlenk and Holtz elaborated that the reaction of diethylzinc and lithium or sodium yields only zinc and an alkali-metal ethylzinc compound; hence, transmetalation does not occur. To favor transmetalation, they employed diorganomercury compounds instead. Nowadays there are many examples of transmetalation reactions involving the $R_2Hg/R'Li$ system,[8] but the $R_2Zn/R'Li$ system normally yields lithium zincates of the general composition $Li_2ZnR_2R'_2$ or $LiZnR_2R'$.[9–11] An unexpected transmetalation reaction of an organolithium compound and dimethyl zinc to give a diorganozinc complex was reported as well.[12]

For a cooperative effect to facilitate alkali-metal-mediated zincation (AMMZ), however, close proximity of the two metal ions is necessary. The degree of aggregation of these novel synthetic reagents can be modulated by the donor solvents as well as the size of the substituents at the zinc atom.[13] The whole ensemble of solvent, donor, and substituents determines whether a solvent-separated ion pair (SSIP) or a contact ion pair (CIP) is formed.[14]

Surprisingly, apart from powder diffraction data of parent $[Li_2ZnMe_4]$,[10] no crystal structure of the basic methyl zincates is available in the current CCDC.[15] Only zincates with bulky substituents (*t*Bu, $SiMe_3$, aryl) at the zinc atom are structurally characterized as SSIPs.[11,16] X-ray crystal structures of zincates as CIPs show four-membered Li-L-L-Zn (L = ligand) rings as the central structural motif, and recently the structure of $[Zn\{(\mu\text{-}Me)_2Li(tmeda)\}_2]$ was determined by Hevia and co-workers.[17] Obviously, the amide ligand tmp plays an important role in bridging the lithium and zinc centers.[18] Like ring stacking and ladder formation in lithium amides,[19] the amide ligand apparently promotes the proximity of the two metals and facilitates the bridging coordination of the alkyl group, although very recent examples were published with two bridging alkyl groups.[20]

Herein we present the results of low-temperature aggregation and deaggregation experiments with the donor bases *N*,*N*,*N*′,*N*′,*N*″-pentamethyldiethylenetriamine (pmdeta) and diglyme. Under otherwise identical conditions, the first gives a CIP of the lithium cation and the $ZnMe_3$ zincate anion, while the latter gives a SSIP with the lithium cation embedded in two diglyme donors (Scheme 1). Both samples were

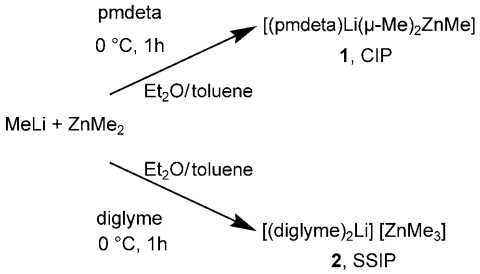

Scheme 1. Syntheses of **1** and **2**.

crystallized at −45 °C from a toluene/diethyl ether solution and mounted on the diffractometer at −100 °C (for details and references see the Experimental Section). At slightly higher temperatures, they decompose rapidly. In the presence of the chelating ligand pmdeta, equimolar ratios of MeLi and $ZnMe_2$ form a contact ion pair with lithium and zinc atoms bridged by two methyl groups in $[(pmdeta)Li(\mu\text{-}Me)_2ZnMe]$ (**1**), clearly corroborating the synergistic effect of the two metals. In contrast, the presence of the chelating ligand

[*] S. Merkel, D. Stern, Dr. J. Henn, Prof. Dr. D. Stalke
Institut für Anorganische Chemie der Universität Göttingen
Tammannstrasse 4, 37077 Göttingen (Germany)
Fax: (+49) 551-39-3459
E-mail: dstalke@chemie.uni-goettingen.de

[**] This work was supported by the Deutsche Forschungsgemeinschaft within the priority program 1178 "Experimental charge density as the key to understanding chemical interactions" and the Chemetall GmbH, Frankfurt and Langelsheim

Supporting information for this article is available on the WWW under http://dx.doi.org/10.1002/anie.200901587.

diglyme gives rise to the SSIP $[(diglyme)_2Li][ZnMe_3]$ (**2**). For the latter, a completely different reactivity pattern can be anticipated.

The contact ion pair **1** crystallizes in the orthorhombic space group *Pbca* (Figure 1). A four-membered LiC_2Zn ring forms the central structural motif. Surprisingly, the two Li–C

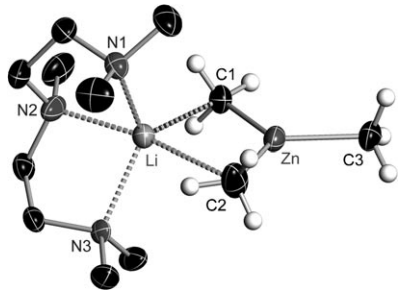

Figure 1. Crystal structure of **1**. Anisotropic displacement parameters are depicted at the 50% probability level. Hydrogen atoms at the donor base are omitted for clarity. Selected bond lengths [pm] and angles [°]: Li–C1 231.9(3), Li–C2 270.6(4),Zn–C1 205.6(2), Zn–C2 203.5(2), Zn–C3 201.8(2), Li–N1 215.1(3),Li–N2 222.7(4), Li–N3 221.8(8); C1-Zn-C2 121.97(8), C1-Zn-C3 119.08(7), C2-Zn-C3 118.94(8).

bond lengths vary considerably. While the Li–C1 distance of 231.9(3) pm is in the normal range for organolithium compounds, the Li–C2 bond of 270.6(4) pm is at the end of that range.[21] Taking these distances in account, it might be anticipated that the shorter bond to C1 has some impact on the Zn–C bonds of the trigonal-planar $ZnMe_3$ moiety. In fact, the shorter Li–C1 bond gives rise to the longest Zn–C1 bond of 205.6(2) pm, compared to the pendant Zn–C3 bond of 201.8(2) pm. Obviously, the competition of two electropositive metals for the electron density of the methanide elongates the zinc–carbon bond. The lithium coordination widens the C1-Zn-C2 angle to 121.97(8)°.

The solvent-separated complex **2** crystallizes in the monoclinic space group $P2_1/c$ (Figure 2). The zinc atom is coordinated by three methyl groups in a trigonal-planar environment. The Zn–C bond lengths are identical within the

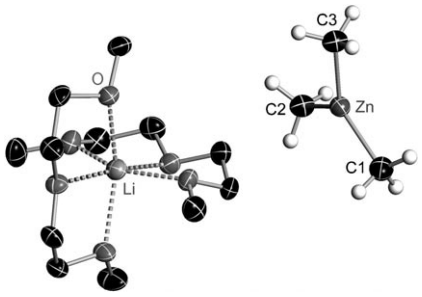

Figure 2. Crystal structure of **2**. Anisotropic displacement parameters are depicted at the 50% probability level. Hydrogen atoms at the donor base are omitted for clarity. Selected bond lengths [pm] and angles [°]: Zn–C1 202.8(5), Zn–C2 203.1(4), Zn–C3 203.4(4), av Li–O 212.2(8); C1-Zn-C2 122.08(18),C1-Zn-C3 121.00(18), C2-Zn-C3 116.91(18).

estimated standard deviations (202.8(5) to 203.4(4) pm). The lithium ion is coordinated by the six oxygen atoms of the two almost orthogonal diglyme molecules, forming a slightly distorted octahedral coordination polyhedron. Obviously, the steric demand of diglyme is smaller than that of pmdeta and permits the coordination of two donor molecules to a single lithium cation. This coordination behavior is typical for diglyme.

The solid-state structures of organometallic compounds obtained from X-ray data do not necessarily correspond to the molecular structures in solution, because different aggregation states might appear in superimposed equilibria.[9b] Therefore, we performed ^{1}H diffusion-ordered NMR spectroscopy experiments (^{1}H DOSY)[22] to gain insight into the structures and aggregation of **1** and **2** in solution.

Whereas for **1** the ^{1}H NMR spectrum shows only one singlet for the protons of the $[ZnMe_3]^-$ ion, indicating the rapid exchange of the CH_3 positions or even an SSIP in solution, the diffusion constants of pmdeta and $ZnMe_3$ were found to be identical ($D = -8.92$), thus demonstrating that the CIP is retained in solution. In contrast, the diffusion constants of the $[(diglyme)_2Li]^+$ ion ($D = -8.73$) and the $[ZnMe_3]^-$ ion ($D = -8.59$) in **2** are different, thus indicating that there is no interaction between the anion and the cation of the SSIP in solution. As expected, the trend of the diffusion constants reflects the size of the aggregates: $[(pmdeta)Li(\mu\text{-}Me)_2\text{-}ZnMe] > [(diglyme)_2Li]^+ > [ZnMe_3]^-$ (Figure 3). Hence,

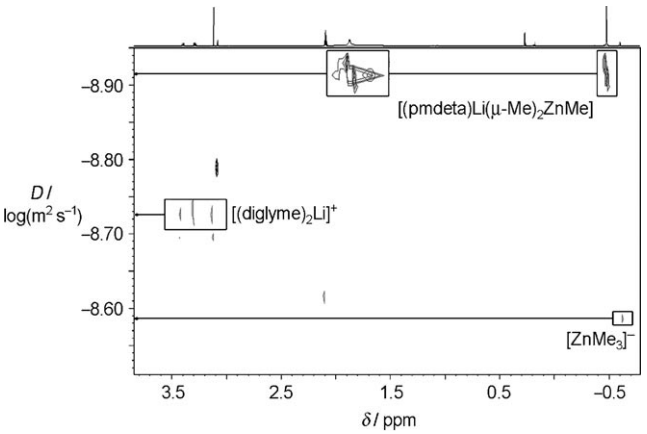

Figure 3. Superposition of ^{1}H DOSY NMR spectra of **1** and **2** showing the diffusion constants *D* in logarithmic scale [$\log(m^2 s^{-1})$].

both DOSY experiments confirm that the structural information from the single crystal diffraction experiments mirrors the aggregation state of zincates **1** and **2** even in solution, which is essential for the prediction of reasonable reactivity patterns.

To characterize the bonding in **1** and to substantiate the Li–C bonding in the CIP, DFT calculations at the B3LYP/TZVP level of theory were performed to optimize its gas-phase structure (for details see Theoretical Section). The results exclude that the contact originates from poorly defined crystal packing effects. A topological analysis of the electron density employing Bader's quantum theory of atoms

in molecules (QTAIM) approach[23] was carried out. This method leads to a network of bond paths (BPs), jointly forming the molecular graph (Figure 4), which in terms of QTAIM can be interpreted as the dominating Lewis structure. In this concept a BP, the path of maximum density between

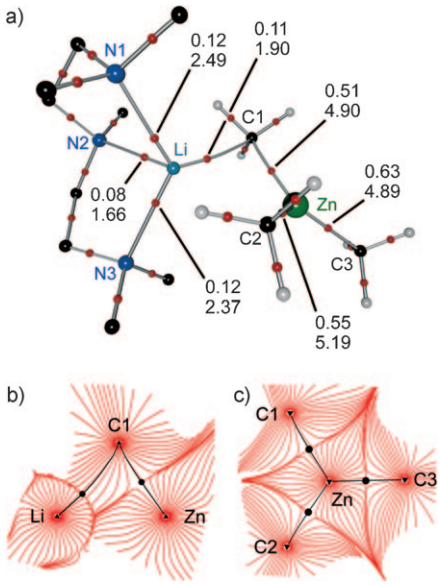

Figure 4. a) Molecular graph of **1** obtained from DFT calculations (B3LYP/TZVP). The small red spheres indicate BCPs, with $\rho(\mathbf{r}_{BCP})$ [eÅ^{-3}] (upper number) and $\nabla^2\rho(\mathbf{r}_{BCP})$ [eÅ^{-5}] (bottom number). Selected bond lengths [pm] and angles [°]: Li–C1 233.3, Li–C2 262.7, Zn–C1 212.2, Zn–C2 209.1, Zn–C3 202.9, Li–N1 224.0, Li–N2 240.5, Li–N3 225.9; C1-Zn-C2 117.23, C1-Zn-C3 118.47, C2-Zn-C3 124.16. b,c) Trajectory plots (red lines) of the Li-C1-Zn plane (b) and the $ZnMe_3$ plane (c). The black lines indicate the bond paths. The black dots indicate the BCPs.

two bonded atoms, is a central quantity to describe the character of a chemical bond.[24] The topological properties of the electron density along the BP provide insight into the bonding situation.[25] The local minimum along the BP is defined as the bond critical point (BCP). The electron density at this point and its derivatives are often utilized to distinguish between various types of atomic interactions.[26]

In an energy-minimized gas-phase structure optimization, the overall molecular graph was reconstructed starting from the crystal geometry, apart from a marginal twist of the $ZnMe_3$ unit. The theoretical Li–C1 bond length (233.3 pm) is close to the experimental distance of 231.9(3) pm, while the Li–C2 bond length of 262.7 pm is even smaller than the experimental value (270.6(4) pm). We found all anticipated BCPs, including that at the Li–C1 bond; however, there is no bond path established between Li and C2. In the computed CIP the Zn–C separations are even more affected by the proximity to the lithium metal than in the crystal structure. While the methyl group at C1 has to share the density with both metals and the Zn–C1 bond is elongated to 212.2 pm, the pendant Zn–C3 bond is about 10 pm shorter.

The topological features of the metal–carbon bonds are in the range anticipated for organometallic compounds: the density at the BCP is relatively low and the Laplacian is positive, indicating a polar bond.[27] The electron density at the Li–C1 BCP of 0.11 e Å^{-3} is approximately as high as at the shorter Li–N donor bonds, hence the bond to preserve the CIP even in solution is as important as a Li–N donor bond, although the donating carbon atom definitely has a lower charge than an amide ligand and is already four-coordinate. The densities at the Zn–C bonds correlate with the distances: the shorter the bond the higher the density. The BCPs of the Li–N and the Li–C bonds are located closer to the lithium atom than to the nitrogen atoms and the carbon atom, reflecting the differences in electronegativity.

Remarkably, in the CIP of parent lithium trimethyl zincate, no additional amide ligand is required to bridge the two metal atoms and to activate the Zn–C bond in the solid state and in solution, as shown by DOSY NMR spectroscopy. The suitable donor base pmdeta leaves a coordination site open and maintains the electronic depletion at the lithium atom. The smaller donor base diglyme gives the SSIP and leaves all Zn–C bonds equal.

Experimental Section

1 and **2:** Pmdeta or diglyme (1.5 equiv) was added to an equimolar solution of dimethylzinc and methyllithium in toluene/Et_2O at 0 °C in inert atmosphere. Crystallization was carried out in a freezer at −45 °C. Yields of crystalline product: 45 % (**1**), 36 % (**2**).

1: ^{1}H NMR (500 MHz, $C_6D_5CD_3$, 25 °C): $\delta = -0.48$ (s, 9H, $(CH_3)_3Zn$), 1.68 (s, br, 8H, CH_2), 1.84 (s, br, 3H, NCH_3), 1.87 ppm (s, br, 12H, $N(CH_3)_2$); ^{13}C{^{1}H} NMR (126 MHz, $C_6D_5CD_3$, 25 °C): $\delta = -6.46$ ($(CH_3)_3Zn$), 44.52 (NCH_3), 45.60 ($N(CH_3)_2$), 54.16 (CH_2), 57.16 ppm (CH_2); ^{7}Li{^{1}H} NMR (194 MHz, $C_6D_5CD_3$, 25°): $\delta = 0.22$ ppm (s); **2**: ^{1}H NMR (500 MHz, $C_6D_5CD_3$, 25 °C): $\delta = -0.60$ (s, 9H, $(CH_3)_3Zn$), 3.11 (s, 12H, (OCH_3)), 3.28 (m, 8H, CH_2), 3.39 ppm (m, 8H, CH_2); ^{13}C{^{1}H} NMR (126 MHz, $C_6D_5CD_3$, 25 °C): $\delta = -7.23$ ($(CH_3)_3Zn$), 58.60 (OCH_3), 70.79 (CH_2), 72.21 (CH_2); ^{7}Li{^{1}H} NMR (194 MHz, $C_6D_5CD_3$, 25 °C): $\delta = 0.05$ ppm (s). Structure analysis of **1** and **2:** The data sets were collected at 100(2) K on a Bruker Smart Apex II with INCOATEC Mo microsource, Apex II detector, and D8 goniometer (**1**) or a Bruker TXS Mo rotating anode with Apex II detector and D8 goniometer (**2**; $Mo_{K\alpha}$ $\lambda = 71.073$ pm) from oil-coated, shock-cooled crystals.[28] The integration was performed with SAINT V7.46A,[29] which was followed by an empirical absorption correction with SADABS-2007/5.[30] The structures were solved by direct methods and refined with SHELXL[31] against F^2.

1: $C_{12}H_{32}LiN_3Zn$, $M = 290.72$ g mol^{-1}, crystal size $0.20 \times 0.20 \times 0.10$ mm^3, orthorhombic, $Pbca$, $a = 12.0040(10)$, $b = 11.3603(10)$, $c = 24.328(2)$ Å, $V = 3317.5(5)$ Å^3; $Z = 8$, $\rho_{calcd} = 1.164$ Mg m^{-3}, $\mu = 1.466$ mm^{-1}, $\theta_{max} = 26.37°$, 39046 reflections measured, 3835 independent reflections, $R_{int} = 0.0317$, $R1 = 0.0292$ [$I > 2\sigma(I)$], $wR2 = 0.0715$ (all data), 0.332/−0.235 e Å^{-3} residual densities.

2: $C_{15}H_{37}LiO_6Zn$, $M = 385.76$ g mol^{-1}, crystal size $0.20 \times 0.10 \times 0.10$ mm^3, monoclinic, $P2_1/c$, $a = 11.428(5)$, $b = 11.695(5)$, $c = 16.897(8)$ Å, $\beta = 108.899(6)°$ $V = 2136.5(17)$ Å^3; $Z = 4$, $\rho_{calcd} = 1.199$ Mg m^{-3}, $\mu = 1.171$ mm^{-1}, $\theta_{max} = 23.81°$, 20157 reflections measured, 3288 independent reflections, $R_{int} = 0.0623$, $R1 = 0.0495$ [$I > 2\sigma(I)$], $wR2 = 0.1233$ (all data), 0.680/−0.535 e Å^{-3} residual densities. CCDC 724370 (**1**) and 724371 (**2**) contain the supplementary crystallographic data for this paper. These data can be obtained free of charge from The Cambridge Crystallographic Data Centre via www.ccdc.cam.ac.uk/data_request/cif.

The quantum chemical calculations for **1** were performed with the TURBOMOLE suite of programs.[32] As Gaussian AO basis, triple-zeta sets of Ahlrichs et al. were employed.[33] In standard notation

these are [3s1p] for H, [5s1p] for Li, [5s3p1d] for C and N, and [6s4p3d] for Zn. A frequency calculation of the lowest Eigenvalues yielded the wavenumbers 21.18, 34.36, 35.97, 52.53, and 56.91 cm^{-1}, which confirms that the optimized structure is in a minimum on the potential-energy surface.

This basis set provides accurate results in DFT optimizations of structures and properties such as the electron density. The geometry has been fully optimized employing C_1 symmetry at the DFT level using the B3LYP hybrid density functional.[34] The electron density obtained by the above procedure was analyzed according to Bader's quantum theory of atoms in molecules (QTAIM)[23] with DGRID[35] and AIM2000[36].

Received: March 23, 2009
Revised: April 29, 2009
Published online: July 20, 2009

Keywords: computational chemistry · electron density · lithium · solvent effects · zincates

[1] a) R. E. Mulvey, *Chem. Commun.* **2001**, 1049; b) R. E. Mulvey, *Organometallics* **2006**, *25*, 1060; c) R. E. Mulvey, F. Mongin, M. Uchiyama, Y. Kondo, *Angew. Chem.* **2007**, *119*, 3876; *Angew. Chem. Int. Ed.* **2007**, *46*, 3802.
[2] J. A. Wanklyn, *Justus Liebigs Ann. Chem.* **1858**, *107*, 125.
[3] a) V. Snieckus, *Chem. Rev.* **1990**, *90*, 879; b) M. C. Whisler, S. MacNeil, V. Snieckus, P. Beak, *Angew. Chem.* **2004**, *116*, 2256; *Angew. Chem. Int. Ed.* **2004**, *43*, 2206.
[4] D. R. Armstrong, W. Clegg, S. H. Dale, E. Hevia, L. M. Hogg, G. W. Honeyman, R. E. Mulvey, *Angew. Chem.* **2006**, *118*, 3859; *Angew. Chem. Int. Ed.* **2006**, *45*, 3775.
[5] P. C. Andrikopoulos, D. R. Armstrong, D. V. Graham, E. Hevia, A. R. Kennedy, R. E. Mulvey, C. T. O'Hara, C. Talmard, *Angew. Chem.* **2005**, *117*, 3525; *Angew. Chem. Int. Ed.* **2005**, *44*, 3459.
[6] H. Naka, M. Uchiyama, Y. Matsumoto, A. E. H. Wheatley, M. McPartlin, J. V. Morey, Y. Kondo, *J. Am. Chem. Soc.* **2007**, *129*, 1921.
[7] W. Schlenk, J. Holtz, *Ber. Dtsch. Chem. Ges.* **1917**, *50*, 262.
[8] a) D. Seyferth, *J. Organomet. Chem.* **1980**, *203*, 183; b) D. Seyferth, *Organometallics* **2006**, *25*, 2; c) D. Seyferth, *Organometallics* **2009**, *28*, 2.
[9] a) E. Rijnberg, J. T. B. H. Jastrzebski, J. Boersma, H. Kooijman, N. Veldman, A. L. Spek, G. van Koten, *Organometallics* **1997**, *16*, 2239; b) T. A. Mobley, S. Berger, *Angew. Chem.* **1999**, *111*, 3256; *Angew. Chem. Int. Ed.* **1999**, *38*, 3070.
[10] E. Weiss, R. Wolfrum, *Chem. Ber.* **1968**, *101*, 35.
[11] M. Westerhausen, B. Rademacher, W. Schwarz, *Z. Anorg. Allg. Chem.* **1993**, *619*, 675.
[12] H. Gornitzka, C. Hemmert, G. Bertrand, M. Pfeiffer, D. Stalke, *Organometallics* **2000**, *19*, 112.
[13] M. Westerhausen, M. Wieneke, W. Ponikwar, H. Nöth, W. Schwarz, *Organometallics* **1998**, *17*, 1438.
[14] C. Lambert, P. von R. Schleyer, *Angew. Chem.* **1994**, *106*, 1187; *Angew. Chem. Int. Ed. Engl.* **1994**, *33*, 1129.
[15] Cambridge Structural Database, v5.30 (November 2008), Cambridge Crystallographic Data Centre, Cambridge, **2008**.
[16] a) K. Thiele, H. Görls, W. Seidel, *Z. Anorg. Allg. Chem.* **1998**, *624*, 555; b) S. R. Boss, M. P. Coles, R. Haigh, P. B. Hitchcock, R. Snaith, A. E. H. Wheatley, *Angew. Chem.* **2003**, *115*, 5751; *Angew. Chem. Int. Ed.* **2003**, *42*, 5593.
[17] D. R. Armstrong, C. Dougan, D. V. Graham, E. Hevia, A. R. Kennedy, *Organometallics* **2008**, *27*, 6063.
[18] H. R. Barley, W. Clegg, S. H. Dale, E. Hevia, G. W. Honeyman, A. R. Kennedy, R. E. Mulvey, *Angew. Chem.* **2005**, *117*, 6172; *Angew. Chem. Int. Ed.* **2005**, *44*, 6018.
[19] a) K. Gregory, P. von R. Schleyer, R. Snaith, *Adv. Inorg. Chem.* **1991**, *37*, 47; b) R. E. Mulvey, *Chem. Soc. Rev.* **1991**, *20*, 167.
[20] a) D. R. Armstrong, E. Herd, D. V. Graham, E. Hevia, A. R. Kennedy, W. Clegg, L. Russo, *Dalton Trans.* **2008**, 1323; b) W. Clegg, J. Garcia-Alvarez, P. Garcia-Alvarez, D. V. Graham, R. W. Harrington, E. Hevia, A. R. Kennedy, R. E. Mulvey, L. Russo, *Organometallics* **2008**, *27*, 2654.
[21] "Lead structures in lithium organic chemistry": : T. Stey, D. Stalke in *The Chemistry of Organolithium Compounds* (Eds.: Z. Rappoport, I. Marek), Wiley, New York, **2004**, p. 47.
[22] a) H. Barjat, G. A. Morris, S. Smart, A. G. Swanson, S. C. R. Williams, *J. Magn. Reson. Ser. B* **1995**, *108*, 170; b) I. Fernández, E. Martínez-Viviente, F. Breher, P. S. Pregosin, *Chem. Eur. J.* **2005**, *11*, 1495.
[23] R. F. W. Bader in *Atoms in Molecules*, Oxford University Press, New York, **1990**.
[24] R. F. W. Bader, *J. Phys. Chem. A* **1998**, *102*, 7314.
[25] R. F. W. Bader, H. Essén, *J. Chem. Phys.* **1984**, *80*, 1943.
[26] a) T. S. Koritsanszky, P. Coppens, *Chem. Rev.* **2001**, *101*, 1583; b) C. Lecomte, M. Souhassou, S. Pillet, *J. Mol. Struct.* **2003**, *647*, 53; c) C. Gatti, *Z. Kristallogr.* **2005**, *220*, 399.
[27] a) P. Macchi, A. Sironi, *Coord. Chem. Rev.* **2003**, *238–239*, 383; b) L. J. Farrugia, C. Evans, M. Tegel, *J. Phys. Chem. A* **2006**, *110*, 7952; c) C. Gatti, D. Lasi, *Faraday Discuss.* **2007**, *135*, 55; d) A. Reisinger, N. Trapp, I. Krossing, S. Altmannshofer, V. Herz, M. Presnitz, W. Scherer, *Angew. Chem.* **2007**, *119*, 8445; *Angew. Chem. Int. Ed.* **2007**, *46*, 8295; e) U. Flierler, M. Burzler, D. Leusser, J. Henn, H. Ott, H. Braunschweig, D. Stalke, *Angew. Chem.* **2008**, *120*, 4393; *Angew. Chem. Int. Ed.* **2008**, *47*, 4321; f) L. J. Farrugia, C. Evans, D. Lentz, M. Roemer, *J. Am. Chem. Soc.* **2009**, *131*, 1251.
[28] a) T. Kottke, D. Stalke, *J. Appl. Crystallogr.* **1993**, *26*, 615; b) D. Stalke, *Chem. Soc. Rev.* **1998**, *27*, 171.
[29] Bruker AXS Inc., *SAINT v7.46A*, Madison, WI, USA, **2007**.
[30] G. M. Sheldrick, *SADABS 2007/5*, Göttingen, **2007**.
[31] G. M. Sheldrick, *Acta Crystallogr. Sect. A* **2008**, *64*, 112.
[32] a) R. Ahlrichs, M. Bär, M. Häser, H. Horn, C. Kölmel, *Chem. Phys. Lett.* **1989**, *162*, 165; b) O. Treutler, R. Ahlrichs, *J. Chem. Phys.* **1995**, *102*, 346; c) K. Eichkorn, F. Weigend, O. Treutler, R. Ahlrichs, *Theor. Chem. Acc.* **1997**, *97*, 119.
[33] A. Schäfer, C. Huber, R. Ahlrichs, *J. Chem. Phys.* **1994**, *100*, 5829.
[34] a) P. A. M. Dirac, *Proc. R. Soc. London Ser. A* **1929**, *123*, 714; b) J. C. Slater, *Phys. Rev.* **1951**, *81*, 385; c) A. D. Becke, *Phys. Rev. A* **1988**, *38*, 3098; d) C. Lee, W. Yang, R. G. Parr, *Phys. Rev. B* **1988**, *37*, 785; e) A. D. Becke, *J. Chem. Phys.* **1993**, *98*, 5648.
[35] M. Kohout, *DGrid*, *Version 4.4*, Radebeul, Germany, **2008**.
[36] F. Biegler-König, J. Schönbohm, D. Bayles, *J. Comput. Chem.* **2001**, *22*, 545.

